**ORIGINAL ARTICLE**

# Curcumin alleviates AFB1-induced nephrotoxicity in ducks: regulating mitochondrial oxidative stress, ferritinophagy, and ferroptosis

Haiyan Liu[1] · Ying He[2,3,4] · Xinglin Gao[1] · Tong Li[1] · Baoxin Qiao[1] · Lixuan Tang[1] · Juan Lan[1] · Qian Su[1] · Zhiyan Ruan[5] · Zhaoxin Tang[1] · Lianmei Hu[1]

## Abstract

Aflatoxin B1 (AFB1), an extremely toxic mycotoxin that extensively contaminates feed and food worldwide, poses a major hazard to poultry and human health. Curcumin, a polyphenol derived from turmeric, has attracted great attention due to its wonderful antioxidant properties. Nevertheless, effects of curcumin on the kidneys of ducks exposed to AFB1 remain unclear. Additionally, the underlying mechanism between AFB1 and ferroptosis (based on excessive lipid peroxidation) has not been sufficiently elucidated. This study aimed to investigate the protective effects and potential mechanisms of curcumin against AFB1-induced nephrotoxicity in ducklings. The results indicated that curcumin alleviated AFB1-induced growth retardation and renal distorted structure in ducklings. Concurrently, curcumin inhibited AFB1-induced mitochondrial-mediated oxidative stress by reducing the expression levels of oxidative damage markers malondialdehyde (MDA) and 8-hydroxy-2 deoxyguanosine (8-OHdG) and improved the expression of mitochondria-related antioxidant enzymes and the Nrf2 pathway. Notably, curcumin attenuated iron accumulation in the kidney, inhibited ferritinophagy via the NCOA4 pathway, and balanced iron homeostasis, thereby alleviating AFB1-induced ferroptosis in the kidney. Collectively, our results suggest that curcumin alleviates AFB1-induced nephrotoxicity in ducks by inhibiting mitochondrial-mediated oxidative stress, ferritinophagy, and ferroptosis and provide new evidence for the mechanism of AFB1-induced nephrotoxicity in ducklings treated with curcumin.

**Keywords** AFB1 · Curcumin · Mitochondrial oxidative stress · Ferritinophagy · Ferroptosis

✉ Lianmei Hu
hulianmei@scau.edu.cn

Haiyan Liu
857479891@stu.scau.edu.cn

Ying He
heying921@163.com

Xinglin Gao
15224349811@stu.scau.edu.cn

Tong Li
lt@stu.scau.edu.cn

Baoxin Qiao
20213073091@stu.scau.edu.cn

Lixuan Tang
tanglixuan@stu.scau.edu.cn

Juan Lan
20202029004@stu.scau.edu.cn

Qian Su
sq@stu.scau.edu.cn

Zhiyan Ruan
ruanzy@gdyzy.edu.cn

Zhaoxin Tang
tangzx@scau.edu.cn

1.  College of Veterinary Medicine, South China Agricultural University, Guangzhou 510642, China

2.  Guangxi Key Laboratory of Veterinary Biotechnology, Guangxi Veterinary Research Institute, Nanning 530001, China

3.  Guangxi Key Laboratory of Veterinary Biotechnology, Nanning, Guangxi, China

4.  Key Laboratory of China (Guangxi)-ASEAN Cross-border Animal Disease Prevention and Control, Ministry of Agriculture and Rural Affairs of China, Nanning, China

5.  School of Pharmacy, Guangdong Food & Drug Vocational College, No. 321, Longdong North Road, Tianhe District, Guangzhou 510520, Guangdong, China

## Introduction

Aflatoxins are a spectrum of toxins produced by *Aspergillus flavus* and *Aspergillus parasiticus*, among which aflatoxin B1 (AFB1) is the most principal component. AFB1 plays a role in toxicity and carcinogenicity and was recognized as a class 1 carcinogen by the Agency for Cancer Research in 1993 (Chuaysrinule et al. 2023; Deng et al. 2022). AFB1 is globally widespread in all types of crops, causing severe contamination. Especially in sub-Saharan Africa, Southeast Asia, and South Asia, AFB1 contamination is most severe, frequently exceeding the maximum European Union regulatory limit in feed (Gruber-Dorninger et al. 2019). Currently, despite the fact that AFB1 level in human food is subject to a certain degree of stringent control, food that does not meet the requirements is frequently diverted to use as animal feed, as the maximum level allowed in animal feed is 300 ppb, which far exceeds the level in human food (Rushing and Selim 2019). This contributes to growth disorders, immunosuppression, and even acute death in humans through the accumulation of AFB1 in the food chain (Malir et al. 2023; Wang et al. 2022b). Therefore, AFB1 contamination is a tremendous socio-economic and health hazard to livestock, poultry, and human beings.

AFB1 enters the animal liver for metabolic activity; subsequently transformed in the kidney (one of the chief target organs of AFB1) or lung, mammary gland, and placenta; and ultimately may evoke immunosuppression, carcinogenicity, teratogenicity, and mutagenicity (Li et al. 2019a; Zhao et al. 2021). In addition, the kidney, with the highest number of mitochondria, is the second largest organ in the body after the heart (Di Paola et al. 2022). Based on the distinctively higher sensitivity to AFB1 compared to other poultry, ducks are used in biological tests to detect feedstuffs (Diaz and Murcia 2019). However, studies on kidney damage in ducks caused by AFB1 remain scarce, and no specific mechanism has been studied.

In the above metabolic process, AFB1-exo-8, 9-epoxide (AFBO), and reactive oxygen species (ROS) produced by AFB1 conversion are the main toxic substances (Benkerroum 2020). AFBO and ROS (oxidative stress causes its accumulation) can react with macromolecules including nucleic acids, proteins, and immune cells, resulting in serious damage to various organs (Wang et al. 2022a). As the main organelle for ROS production, mitochondria regulate many biochemical processes, such as redox homeostasis and iron metabolism (Dard et al. 2020). Meanwhile, mitochondrial oxidative stress is closely related to ferroptosis, an iron-dependent form of programmed cell death, which is closely associated with kidney injury and is considered a new therapeutic target for kidney disease (Bayir et al. 2023). Nevertheless, the role and mechanism of ferroptosis in the poisoning of ducklings by AFB1 have not been reported so far, and further research is urgently needed to find an effective solution to AFB1 poisoning.

Techniques are developed to detoxify AFB1, including chemical reagent oxidation, hydrolytic enzymes, microorganisms, and heat treatment (Nazhand et al. 2020), among which phytochemicals are particularly popular due to very low toxicity and few side effects (Fan et al. 2021b). Up to now, no specific drug for AFB1 detoxification has been found yet. Adedara and Owumi found that an artemisinin-based drug alleviates low doses of AFB1 poisoning but was ineffective when AFB1 doses up to 70 µg/kg body weight (BW) (Adedara and Owumi 2023). Curcumin, a polyphenolic compound derived from the rhizome of the plant turmeric, has antioxidant, anti-inflammatory, antifungal, and hypolipidemic properties and is often used by humans as a coloring agent and food additive (Mohajeri et al. 2018). ALTamimi et al. reported that the addition of curcumin into the diet of diabetic rats activates Nrf2 and improves the antioxidant capacity to prevent kidney injury (ALTamimi et al. 2021). In addition, curcumin was also found to attenuate rhabdomyolysis-induced acute kidney injury in mice by inhibiting ferroptosis (Guerrero-Hue et al. 2019). Despite the protective effect of curcumin on kidney damage in mice, the effects of curcumin on AFB1-induced nephrotoxicity and its underlying mechanisms remain unclear.

The objective of the present study was to explore possible new mechanisms of AFB1 damage to duck kidneys and the potential therapeutic effects of curcumin and further provide a reference for the detoxification of AFB1, the protection of animal health, and the reduction of economic losses.

## Materials and methods

### AFB1 and curcumin

AFB1 was purchased from Shanghai Macklin Biochemical Co. Ltd. (China). Curcumin was purchased from Nutri Herbal Biotechnology Co. Ltd. (Nanjing, China).

### Animal and experimental treatment

Purchased from Huimin Poultry Industry Co. Ltd. (Guangzhou, China), a total of forty single-day-old ducklings were selected to conduct the pre-experiment. All ducklings were reared in cages with ambient conditions (20–26 °C, relative humidity between 45 and 65%, 12-h light-dark cycle). After 1 week of acclimation, the ducklings were then randomly divided into four groups ($n=10$ per group): control (basal diet), L-CUR (base diet mixed with 200 mg/kg curcumin), M-CUR (base diet mixed with 400 mg/kg curcumin), and

H-CUR (base diet mixed with 600 mg/kg curcumin). The dose of curcumin was determined based on previous trials (Ruan et al. 2019). After the course of the 30-day experiment, all ducks were euthanized with sodium pentobarbital, and the kidney tissue samples were collected at – 80 °C or paraformaldehyde for follow-up experiments.

Curcumin 400 mg/kg dose was chosen as the treatment group since pre-experimental results revealed that it had the most pronounced benign effect on ducks. Thence, thirty ducklings were purchased to investigate the effect of AFB1 and curcumin treatment. In the formal experiment, ducklings were randomly and equally divided into three groups: control (1% dimethyl sulfoxide for 1 mL/kg BW), AFB1 (0.1 mg/kg BW AFB1), and CUR + AFB1 (0.1 mg/kg BW AFB1 and 400 mg/kg curcumin). AFB1 was administered by gavage for 21 days, and all preliminary preparations, rearing environment, and operation were the same as the pre-experiment. The dose of AFB1 was determined based on our previous trials (Ruan et al. 2019; Wan et al. 2022). All animal treatments and experimental procedures were confirmed by the Institutional Animal Care and Ethics Committee of South China Agricultural University (Permit Number: 2020A004).

## Body weight and kidney coefficient

The weight of the ducks was recorded daily. The final body mass combined with the corresponding renal quality was obtained subsequently to calculate the kidney coefficient by applying the following formula: kidney index = kidney weight (g)/body weight (g) × 100%.

## Histopathological examination

Kidney tissues fixed in 4% paraformaldehyde were trimmed into small flat squares and then flushed overnight with running water. Embedded in paraffin wax, kidney blocks were made into thin paraffin sections of 4 μm thickness and performed on hematoxylin and eosin (HE) staining. Masson staining was carried out in accordance with the manufacturer's instructions (abs9347, Absin, China). At length, the images of slices sealed with neutral resin and dried were taken under a light microscope with a tenfold objective for inspection.

## Detection of Fe and MDA levels

Tissue Iron Content Assay Kit (BC4350, Solarbio, China) was utilized to measure iron content in kidneys with a visible spectrophotometric method. MDA assay kit (TBA method) (A003-1, Nanjing Jiancheng Bioengineering Institute, China) was chosen to perform the quantitative testing for MDA. All procedures were carried out as per the manual.

## Quantitative real-time PCR analysis (RT-qPCR)

The total RNA of the kidney was extracted by TRIzol reagent (Takara, Japan). For the next step, the uniform concentration of RNA harvested was removed from DNA and reverse transcribed to cDNA with the HiScript® III RT SuperMix for qPCR (Vazyme, China) following the instructions. Real-time quantitative reverse transcription reaction was run on the fluorescent quantitative PCR instrument (LightCycler 480, Roche, Germany) with ChamQ Universal SYBR qPCR Master Mix (Vazyme, China). GAPDH and β-tubulin were reference genes used for normalization. The specific sequences of upstream and downstream primers are listed in Table 1.

## Western blotting analysis

In order to adequately lyse the tissue to release the proteins therein, kidney tissue samples were immersed in the solution equipped with RIPA and PMSF (Beyotime, China) at a 100-to-1 ratio. Protein concentration was examined with a BCA protein assay kit (Vazyme, China) and uniformly concentrated to 1 mg/mL, followed by aspiration of 9 μL for sodium dodecyl sulfate-polyacrylamide gel electrophoresis and transferred to a methanol-activated polyvinylidene fluoride membrane. Blocked with 5% skimmed milk powder, the membranes were incubated in primary antibodies overnight in a 4 °C refrigerator prior to the horseradish peroxidase (HRP)-labeled secondary antibody for 1 h at room ambient temperature (IgG; 1:5000, CWBIO, Beijing, China). Protein blotting on the membrane was revealed by a gel imaging system (Biolight, China) scanning with enhanced chemiluminescence (ECL) kits (Vazyme, China) and analyzed grayscale value via ImageJ software (National Institutes of Health, DC, USA). Primary antibodies are shown in Table 2.

## Immunohistochemistry and immunofluorescence staining assay

The dewaxed and rehydrated kidney paraffin sections were subject to antigen repair and then were conducted with immunohistochemistry and immunofluorescence staining to detect the protein expressions of 8-OHdG, Nrf2, SOD, GPX4, FTL, and LC3.

## Statistical analysis

Acquired from no fewer than three independent tests, all the data are displayed as mean ± SEM. For demonstrating the comparison between groups, Student's $t$-test was utilized and implemented with GraphPad Prism 8.01 (GraphPad Software, San Diego, CA, USA). The results were considered to have significant differences when $P < 0.05$.

**Table 1** Primers used for RT-qPCR

| Gene | Forward primer (5′–3′) | Reverse primer (5′–3′) |
| --- | --- | --- |
| Nrf2 | AAGCCCTGAAACCAAGTCAA | AGGGCTCTCAACAGTCTCCA |
| Keap1 | CATCAATTGGGTGCAGTACG | AGCACTTGGGTGGGTTTATG |
| GPX-1 | ACCAACCCGCAGTACATCAT | AGCCTCCTTGGGGACTTTCT |
| CAT | CTGTTTGAGGAAGCAGGAAG | GAAAGACCAGGATGGGTAGTTG |
| HO-1 | AAACTTCCCAGAAACACGG | CCGTTCTCCTGGCTCTTT |
| SOD-1 | CCTGTGGTGTCATCGGAATA | TTGAACGAGGAAGAGCAAG |
| Trx | CATGGTGTGGACCATGCAAA | TCGATGAACACCACATCCCC |
| Trx2 | ACGATCACACAGACCTTGCC | ACGTCTCCGTTCTTCATGGC |
| SOD2 | TACGACTATGGCGCTCTGGA | TTGTTGACATATGCGGCGTG |
| Prdx3 | CTGGCATAGCACTGAGAGGT | TCTCCATGCGTCTCCACGTA |
| Grx3 | GGCCCAGCTATCATTAGGAGA | TGGTGCACTGGATTAAGGTTT |
| P62 | GAAGCGGATCCTCGCTTGAT | GCAGAAGTCGAGTGAGCCAT |
| LC3A | TCCTTGTCCCAGACCATGTC | GCCATCCTCATCCTTCTCCT |
| LC3B | TGAAGTGTAGCAGGATGCGA | GAGTGCCAAGACGCAGTAGT |
| Beclin-1 | GGCCAATAAGATGGGTCTGA | GCTACCATTGCATGGTCAAA |
| ACSL4 | GACATCTGCTCGGGACTGAC | GCAAGAGCAAAAGCAGCAGT |
| TF | ACAGCCTAAAGGACCACACG | CTCTGGCCCAGTTACACGTT |
| COX2 | TCCACCAACAGTGAAGGACA | CGACCAAGCCAAACACCTC |
| AIFM2 | ACGAGAACATCTACGCCGTC | GCTTGTGTGTCAGGCTGTTG |
| GPX4 | GACGGCAACGATGTGAGC | CCCAGGATGCGTAAACCC |
| TFR1 | CTTCGCCACATCTTCTTC | TTCCAAATATCACCCTCTAA |
| NCOA4 | GTTCTCCCAAAGTCTGTTAT | GTCCACCTCTTCTTGTTCC |
| FTH1 | CTACTACTTTGACCGGGATG | CCATTCTCCCAGTCATCAC |
| GAPDH | GAGGGTAGTGAAGGCTGCTG | CACCACACGGTTGCTGTATC |

**Table 2** Primary antibodies

| Protein | Dilution ratio | Company | Country |
| --- | --- | --- | --- |
| GAPDH | 1:1500 | Bioss | China |
| Keap1 | 1:1000 | Bioss | China |
| HO-1 | 1:1000 | Abcam | USA |
| AIFM2 | 1:2000 | Proteintech | China |
| Nrf2 | 1:1000 | Bioss | China |
| Trx | 1:1000 | Bioss | China |
| TF | 1:1000 | Proteintech | China |
| TFR | 1:1000 | Proteintech | China |
| GPX4 | 1:1000 | Bioss | China |
| NCOA4 | 1:1000 | Bioss | China |
| LC3 | 1:1000 | Sigma-Alorich | USA |
| P62 | 1:2500 | Proteintech | China |
| Beclin1 | 1:500 | Novus Biologicals | USA |
| FTH1 | 1:1000 | Affinity | China |
| FTL | 1:1000 | Proteintech | China |
| SLC7A11 | 1:1000 | Bioss | China |
| ACSL4 | 1:1000 | Affinity | China |
| COX2 | 1:1000 | Bioss | China |

# Results

## Effect of curcumin gradient treatment

Initially, we examined the effects of 200 mg/kg, 400 mg/kg, and 600 mg/kg curcumin-alone administration on body weight and kidneys of ducks. Compared to the control group, the body weight of ducklings in the M-CUR group was dramatically higher ($P < 0.05$) while that of ducklings in the L-CUR and H-CUR groups showed no obvious change (Fig. 1A). Meanwhile, from the 10th day onwards, ducklings in the M-CUR group grew faster compared with the other three groups (Fig. S1). Additionally, we observed and analyzed the renal coefficients, appearance, and pathological sections, yet no significant difference was found (Fig. 1B–D). Accordingly, we adopted 400 mg/kg as the treatment group for the subsequent trial.

## Effects of body weight and kidney index

In the process of feeding, the variance in body weight of the three experimental groups of ducks emerged over time which was clearly reflected in the growth graph (Fig. 2A). Ducks treated with AFB1 were lighter than those with CUR on the 11th day and much lighter than those in the control group furthermore on the 21st day ($P < 0.05$ or $P < 0.01$). Meanwhile, Fig. S2 showed that curcumin was able to alleviate
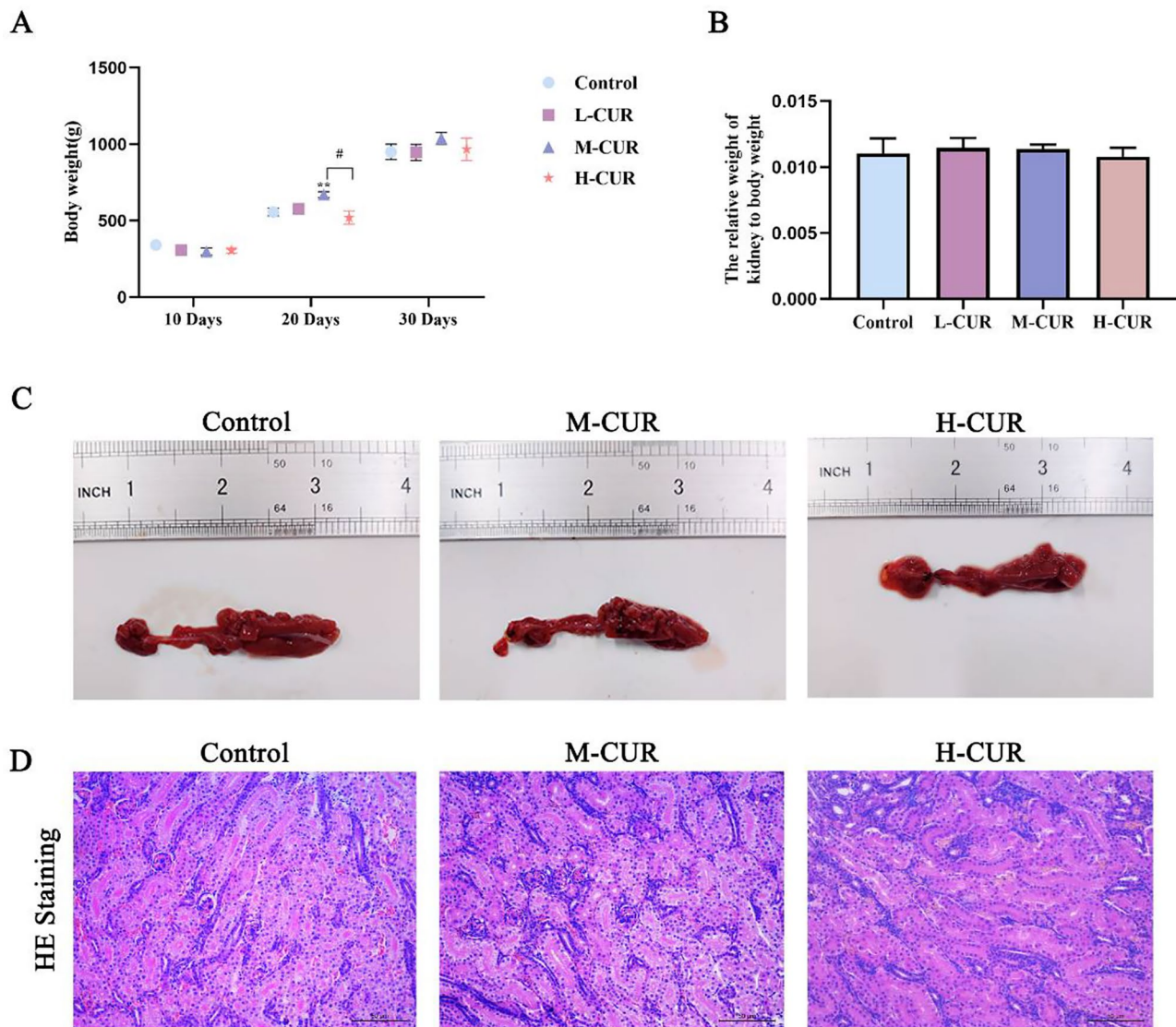
Fig. 1 Effects of different concentrations of curcumin treatment on body weight and kidney. **A** Body weight changes of ducks in consequent 30 days. **B** Kidney index. **C** The appearance of the kidneys. **D** Duck k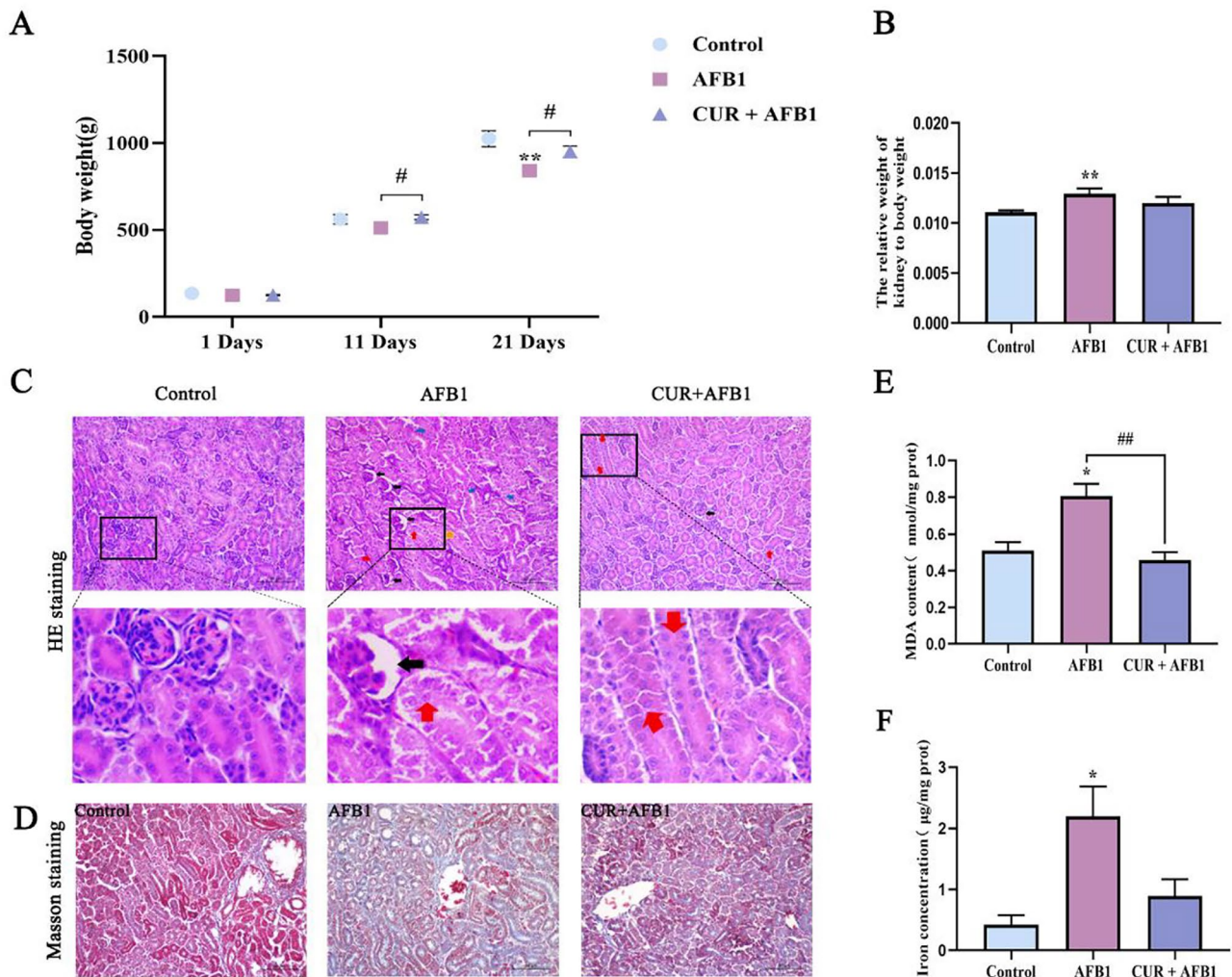idney histological structure (×200). All data were expressed as mean ± SEM; $n=6$ for each group. "*" indicates statistically significant difference from the control group (*$P<0.05$, **$P<0.01$, and ***$P<0.001$). "#" means that the group is significantly different from the M-CUR group (#$P<0.05$, ##$P<0.01$, and ###$P<0.001$)

AFB1-induced low growth rate in ducklings. On the last day of the trial, the kidney index was remarkably higher after receiving AFB1 for handling contrast with the drug-free group ($P<0.01$), as shown in Fig. 2B. These results indicated that AFB1 negatively affected the growth and development of ducks, but curcumin mitigated it to some extent.

## Histopathological injury

In relevance to renal HE and Masson staining, normal glomerular size and tubular structure were seen in the control group. Contrariwise, the AFB1 group exhibited a series of kidney injuries: glomerular wrinkling, capsular dilatation, tubular epithelial cell rupture, nucleus detachment, and tubular dilatation. In the CUR + AFB1 group, renal lesions were significantly reduced with only slight glomerular atrophy and nuclear detachment of tubular epithelial cells (Fig. 2C). Also, Masson-positive areas were notably enlarger in the AFB1 group, indicating a worse fibrotic injury provoked by AFB1 (Fig. 2D). These results suggested that AFB1 caused renal damage and could be alleviated by curcumin.

**Fig. 2** Effects of AFB1 exposure and CUR treatment on weight, kidney, the level of MDA, and iron accumulation. **A** Body weight changes of ducks in consequent 21 days. **B** Kidney index. **C** HE staining of kidneys (×200). Black arrow: glomerular crumpling and capsular dilatation; blue arrow: tubular epithelial cell rupture; red arrow: nucleus detachment of tubular epithelial cell; asterisk: tubular dilatation. **D** Masson staining of kidneys (×200). **E** The level of MDA in kidneys. **F** Iron concentration in kidneys. All data were expressed as mean ± SEM; $n = 6$ for each group. "*" indicates statistically significant difference from the control group (*$P < 0.05$, **$P < 0.01$, and ***$P < 0.001$). "#" means that the group is significantly different from the AFB1 group (#$P < 0.05$, ##$P < 0.01$, and ###$P < 0.001$)

## MDA levels and Fe content in kidney

As we can see in Fig. 2E, compared to normally raised ducks, the accumulation of MDA rose conspicuously in the AFB1 group but made a difference in the CUR + AFB1 group ($P < 0.01$ or $P < 0.05$).

Iron overload is one of the characteristics of ferroptosis (Chen et al. 2021). Given the essential role of Fe in ferroptosis, the iron content in kidney tissue was meticulously evaluated via a reagent kit and is explicitly shown in Fig. 2F. Following the gavage of AFB1, iron levels in the kidney elevated sharply ($P < 0.05$). Conversely, the symptom was in remission in the CUR + AFB1 group.

## Effects of mitochondrial oxidative stress in the kidney tissues of ducklings

With respect to oxidative stress, mitochondria are a pivotal part of that. As shown in Fig. 3A–D, the mRNA expression of Prdx3, Trx2, and SOD2 and protein expression of Grx3, Prdx3, and SOD2 rose after AFB1 administration, which exhibited a decline following curcumin treatment except for mRNA expression of SOD2 ($P > 0.05$, $P < 0.01$, $P < 0.001$, $P < 0.0001$). The mRNA expression of Grx3 dropped dramatically in the AFB1 group but rebounded in the CUR + AFB1 group ($P < 0.05$). The inconsistency between gene expression and protein expression of Grx3 may be attributed to post-transcriptional regulation.
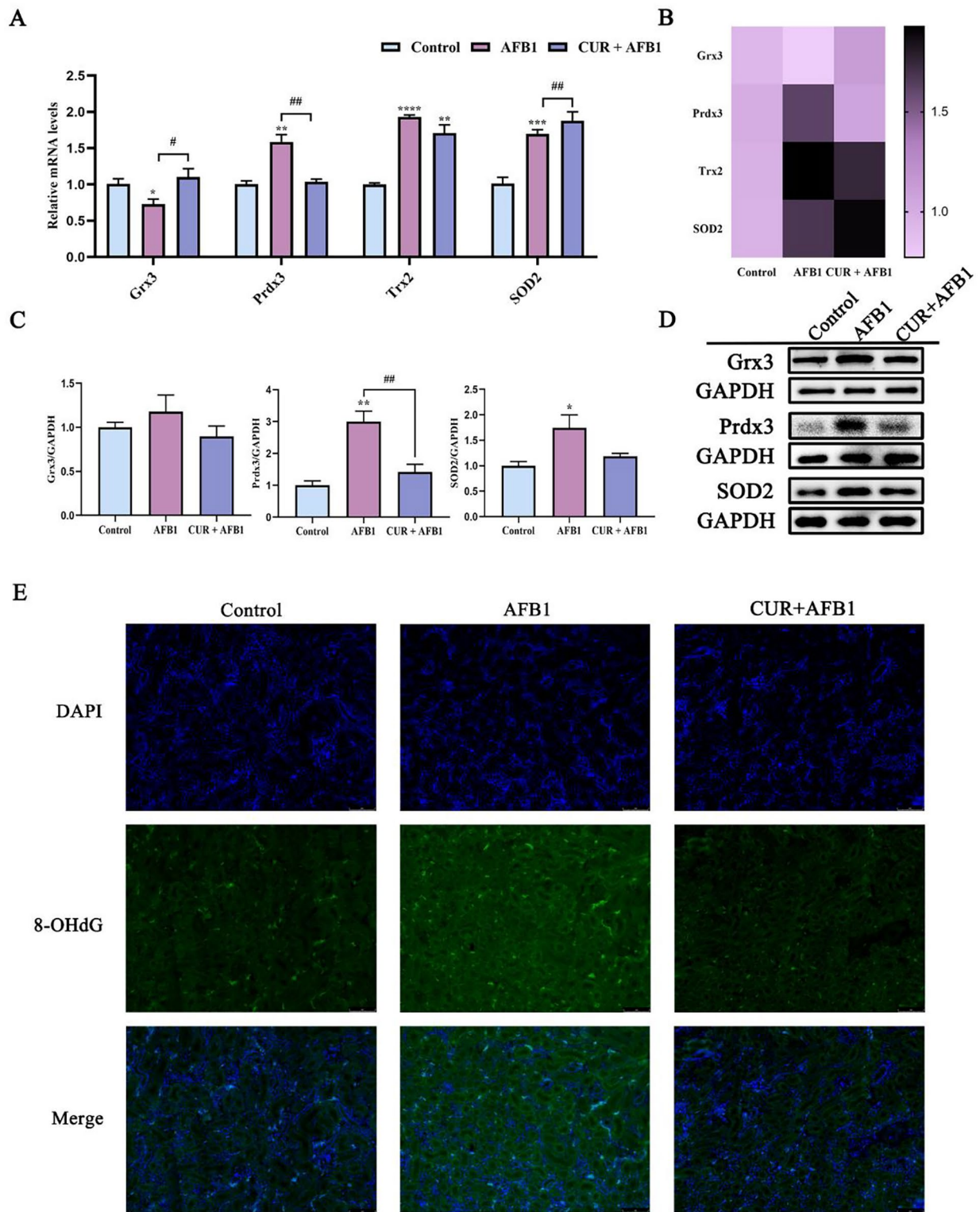
**Fig. 3** Effects of AFB1 exposure and CUR treatment on mitochondrial oxidative stress. **A** mRNA levels of related genes of mitochondrial oxidative stress. **B** Heatmap shows the correlation expression of related genes of mitochondrial oxidative stress. **C** Quantification of protein levels of Grx3, Prdx3, Trx2, and SOD2. **D** Protein bands of Grx3, Prdx3, and SOD2. **E** Immunofluorescence staining for 8-OHdG in duck kidneys ($\times 200$). All data were expressed as mean$\pm$SEM; $n=6$ for each group. "*" indicates statistically significant difference from the control group ($*P<0.05$, $**P<0.01$, $***P<0.001$, and $****P<0.0001$). "#" means that the group is significantly different from the AFB1 group ($\#P<0.05$, $\#\#P<0.01$, $\#\#\#P<0.001$, and $\#\#\#\#P<0.0001$)

Additionally, higher density fluorescence of 8-OHdG was detected in the AFB1 group than in the control group manifested in the immunofluorescence assay, whereas it rebounded in the CUR + AFB1 group (Fig. 3E).

## Effects of Nrf2 signaling pathway in the kidney tissues of ducklings

As depicted in Fig. 4A–D, AFB1 facilitated the mRNA and protein expression of Nrf2 and its downstream target product, such as CAT, GPX1, Trx, and HO-1, which were eased by the addition of curcumin ($P < 0.05$, $P < 0.01$, or $P < 0.001$). However, the mRNA expressions of Keap-1 and SOD and the protein expressions of Keap-1 were apparently downregulated by AFB1 but rose instead after adding curcumin ($P < 0.05$, $P < 0.01$, $P < 0.001$, or $P < 0.0001$). Heatmap illustrated the expression levels of the Nrf2 signaling pathway after different treatments (Fig. 4B).

The immunohistochemistry experiment was applied to facilitate the observation of the results. In Fig. 4E, we can visually see an expanded darker tan positive area of Nrf2 in AFB1-treated kidney than in the control or CUR + AFB1 group. The result of SOD was exactly the opposite (Fig. 4E, F).

## Effects of the ferroptosis-relative index in the kidney tissues of ducklings

Upon the discovery that iron content in the kidney is boosted by the effects of AFB1, we further examined ferroptosis-relative factors. The precipitous reduction of TF, GPX4, and FSP1 mRNA expression caused by AFB1 was eliminated by curcumin (Fig. 5A, B) ($P < 0.05$, $P < 0.01$). On the contrary, the expressions of TFR, ACSL4, COX2, and FTL in ducks disposed of AFB1 were more intense than that by curcumin or no drug ($P > 0.05$, $P < 0.05$, $P < 0.01$, or $P < 0.001$), which was lucidly mirrored by the outcome of RT-qPCR (Fig. 5A, B). Heatmap illustrated the RNA expression levels ferroptosis-relative index after different treatments (Fig. 5B).

The results above were in agreement with what was shown by the western blot presented in Fig. 5C, D, except for TF and FSP1. The hysteresis between transcription and protein formation or post-transcriptional regulation might be an explanation for this. Protein band displayed that SLC7A11 was less expressed in the AFB1 group and further decreased after curcumin treatment ($P < 0.01$, $P < 0.001$).

A crystal clear view captured by immunohistochemistry experiments and immunofluorescence showed that the protein expression of GPX4 in kidneys of ducks exposed to AFB1 had a lower level than the normally treated ducks, while the protein expression of FTL showed the opposite result (Fig. 5E, F).

## Effects of the ferritinophagy-relative index in the kidney tissues of ducklings

Ferritinophagy is an important pathway that gives rise to ferroptosis. Figure 6A, B depicts that mRNA levels of NCOA4, FTH1, LC3A, LC3B, and Beclin1 rose to varying degrees after treatment with AFB1 but declined when AFB1 and curcumin were combined while that of p62 was precisely opposite ($P < 0.05$, $P < 0.01$, $P < 0.0001$). Heatmap illustrated the RNA expression levels of the ferritinophagy-relative index after different treatments (Fig. 6B).

In parallel, as Fig. 6C, D illustrated, protein expressions of NCOA4, LC3B, Beclin1, and p62 noticeably elevated in the AFB1-attack group compared to the control group and then declined in the CUR + AFB1 group compared to the AFB1 group ($P < 0.05$, $P < 0.01$, $P < 0.0001$).

Immunofluorescence results showed an increase in LC3 expression in the AFB1 group as compared to the control group and the CUR + AFB1 group (Fig. 6E).

## Discussion

With the current trend of global warming, AFB1 contamination is increasingly found in foods, causing harm to animals (Fouche et al. 2020; Jallow et al. 2021). Although some previous studies have found that AFB1 induces oxidative stress, inflammation, and autophagy in ducks (Qiao et al. 2023; Wan et al. 2022; Wang et al. 2023), these studies did not fully explain the mechanism of AFB1 toxicity. In this study, it was found that mitochondrial oxidative stress and ferroptosis induced by AFB1 may play an important role in the nephrotoxicity of ducklings and that curcumin may have a good therapeutic effect on it. To our knowledge, this is the first study to reveal AFB1-induced ferroptosis in ducklings and its specific mechanism.

In this study, curcumin-alone treatments were found to have no toxic effect on ducks and had good food source safety and growth promotion. Ducks exposed to AFB1 showed growth inhibition with elevated kidney coefficients, which might be influenced by weight loss, suggesting possible kidney swelling. It was reported that AFB1 induced nutritional deficiencies via reducing the body's ability to absorb nutrients (Gong et al. 2004; Rushing and Selim 2019). That may take on the responsibilities. Liu et al. also found that consumption of AFB1-contaminated cottonseed meal increases liver, kidney, and spleen mass in ducklings, which is in agreement with our finding (Liu et al. 2017). Importantly, the growth inhibition was reversed by curcumin. Curcumin also alleviated the pathological phenomena of glomerular wrinkling, tubular dilatation, and renal tissue fibrosis in AFB1-toxic ducks. Thus, curcumin mitigated
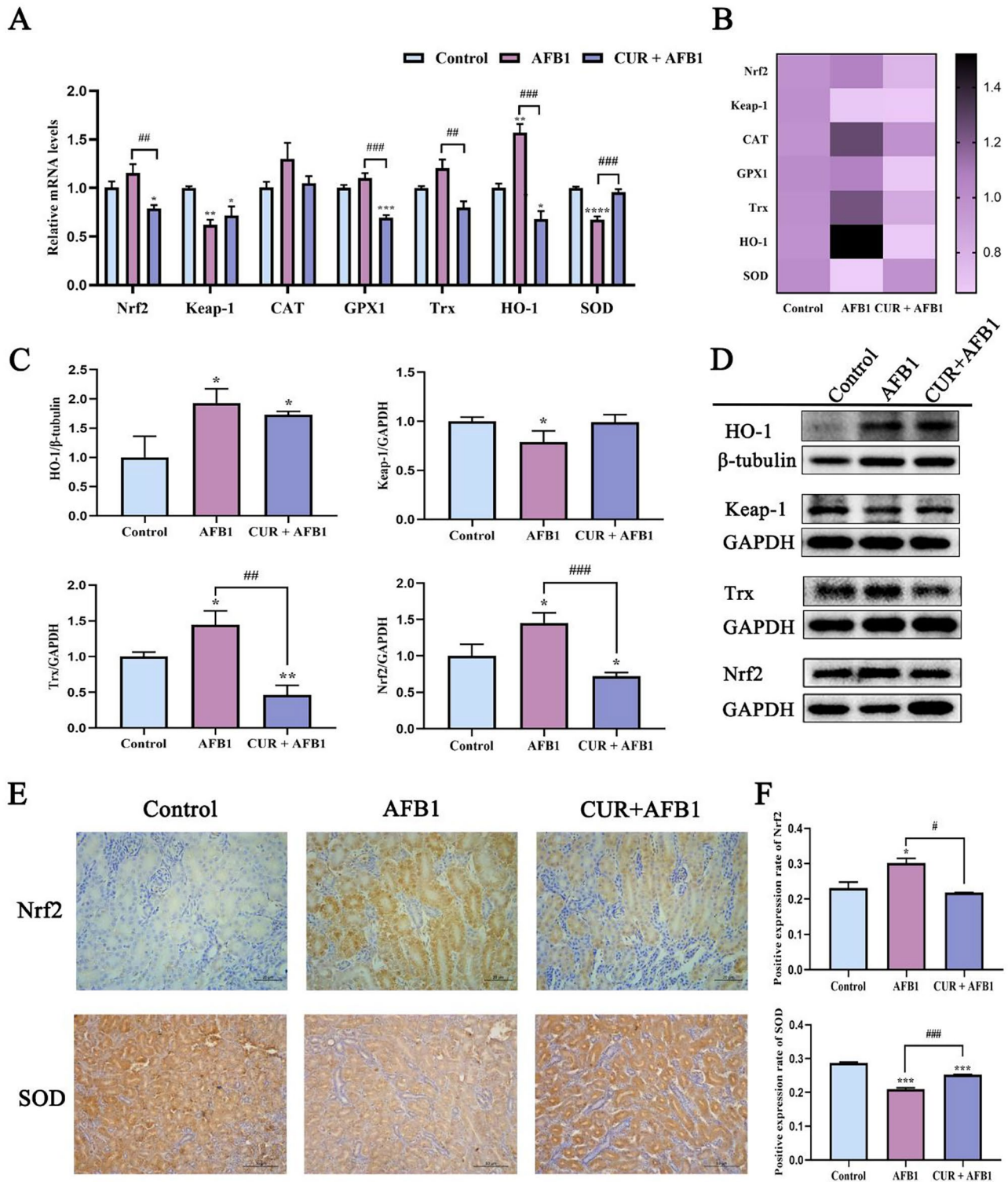
**Fig. 4** Effects of AFB1 exposure and CUR treatment on Nrf2 signaling pathway. **A** mRNA levels of related genes of Nrf2 signaling pathway. **B** Heatmap shows the correlation expression of related genes of Nrf2 signaling pathway. **C** Quantification of protein levels of HO-1, Keap-1, Trx, and Nrf2. **D** Protein bands of HO-1, Keap-1, Trx, and Nrf2. **E** Immunohistochemistry staining analysis for the expression of Nrf2 ($\times 400$) and SOD ($\times 200$) proteins in duck kidneys. All data were expressed as mean $\pm$ SEM; $n = 6$ for each group. "*" indicates statistically significant difference from the control group (*$P < 0.05$, **$P < 0.01$, ***$P < 0.001$, and ****$P < 0.0001$). "#" means that the group is significantly different from the AFB1 group (#$P < 0.05$, ##$P < 0.01$, ###$P < 0.001$, and ####$P < 0.0001$)
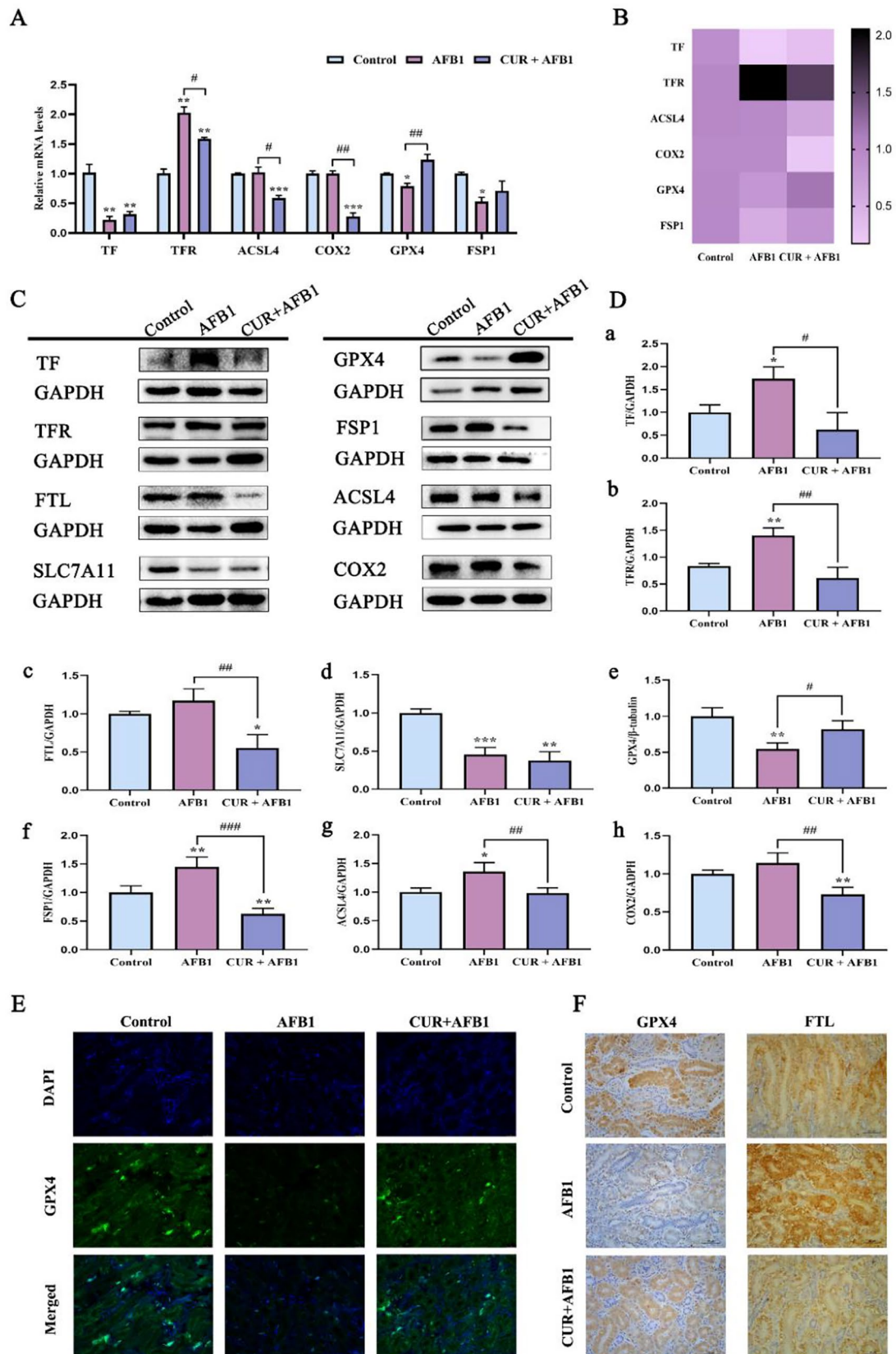
◄ **Fig. 5** Effects of AFB1 exposure and CUR treatment on ferroptosis. **A** mRNA levels of ferroptosis-related genes. **B** Heatmap shows the correlation expression of ferroptosis-related genes. **C** Protein bands of ferroptosis-related genes. **D (a-h)** Quantification of protein levels of ferroptosis-related genes. **E** Immunofluorescence staining for GPX4 in duck kidneys (×400). **F** Immunohistochemistry staining analysis for the expression of GPX4 and FTL proteins in duck kidneys (×200). All data were expressed as mean ± SEM; $n = 6$ for each group. "*" indicates statistically significant difference from the control group (*$P < 0.05$, **$P < 0.01$, ***$P < 0.001$, and ****$P < 0.0001$). "#" means that the group is significantly different from the AFB1 group (#$P < 0.05$, ##$P < 0.01$, ###$P < 0.001$, and ####$P < 0.0001$)

AFB1-induced growth retardation and kidney damage in ducks.

There were pieces of evidence that AFB1 can cause intracellular oxidative/antioxidative imbalance and induce oxidative stress to produce oxidative damage (Wang et al. 2022c; Yu et al. 2018). In our study, 8-OHdG, a marker of oxidative DNA damage, was increased in AFB1-toxic ducks. Subsequently, we found an accumulation of MDA, the end product and marker of lipid oxidation. These results suggest the occurrence of lipid peroxidation and were consistent with the findings of Li et al. on AFB1-poisoned broilers (Li et al. 2019b). Of note, the Nrf2/HO-1 antioxidant signaling pathway was found to be activated, which was different from previous studies that found that AFB1 can inhibit the Nrf2 pathway. We speculate that at this point, the cells were still in a state of active resistance to AFB1-induced oxidative damage, which also suggests that AFB1 triggered oxidative stress in the duckling kidney. Likewise, Fan et al. found that cadmium consistently activated Nrf2, exacerbated oxidative stress, and thereby induced kidney injury (Fan et al. 2021a). The antioxidant system composed of various antioxidant enzymes such as SOD2, Prx3, Trx2, and Grx3 in mitochondria is an important part of cellular defense against oxidative stress (Zhu et al. 2022). Li et al. found that insulin increased the expression levels of mitochondrial antioxidant proteins (GPX4, Grx3, Prdx3, Trx2) and activated the mitochondrial antioxidant pathway in the kidney of diabetic dogs (Li et al. 2022). In our study, the levels of SOD2, Prx3, and Trx2 all increased after AFB1 treatment, which suggests that AFB1 induced mitochondrial oxidative stress in the kidney of ducks. Additionally, the declined expression of Grx3 and SOD indicates that the activated antioxidant system was no longer adequately able to defend against oxidative damage, which is consistent with previous findings (Ma-On et al. 2017). Importantly, curcumin treatment reversed all these conditions and attenuated the mitochondrial-mediated oxidative stress in duck kidneys, which was probably a credit to its antioxidant properties and also validated the previous statement.

Mitochondria are involved in iron metabolism, ROS production, and redox homeostasis and are found to be the ultimate step in ferroptosis (Gao et al. 2019; Oh et al. 2022).

Chen et al. have proved that mitochondrial oxidative stress mediates Fe-induced ferroptosis via the Nrf2-ARE pathway (Chen et al. 2022). In this study, we found that AFB1 caused lipid peroxidation, which is one of the traits of ferroptosis. Thus, we further explored whether there was an occurrence of ferroptosis. The results showed that AFB1 did cause considerable iron accumulation in the duck kidney. Chen et al. reported that almost all circulating iron is transported into the cell and thus involved in ferroptosis by binding to the plasma glycoprotein TF/TFR (Chen et al. 2021). Xie et al. found that TF/TFR-induced oxidative stress and iron overload have been found to exacerbate ferroptosis after intracerebral hemorrhage (Xie et al. 2023). Intriguingly, in the present research, AFB1 also elevated the expressions of TFR and TF. Meanwhile, iron taken up by cells is stored in ferritin composed of ferritin heavy chain (FTH) and ferritin light chain (FTL), both of which we detected a pronounced upward trend in expression after AFB1 disposal in our study. These results indicate that AFB1 enhanced cellular iron intake and elicited iron accumulation.

As for the pathway of resistance to ferroptosis, the system xc⁻ consisting of SLC7A11 and SLC3A2 participates in the synthesis of glutathione (GSH) by transporting cystine. GPX4 is an important regulator of resistance to ferroptosis, which can inhibit ferroptosis by converting lipid hydroperoxides to lipid alcohols and reducing ROS production (Zhuang et al. 2022; Yang et al. 2014). Our research found that AFB1 significantly downregulated GPX4 and SLC7A11 and restrained the system xc⁻/GSH/GPX4 axis, the extremely crucial anti-ferroptosis pathway. Additionally, cyclooxygenase-2 (COX2) and acyl-coenzyme A synthetase long-chain family member 4 (ACSL4), as markers of ferroptosis that can catalyze lipid peroxide formation, were both upregulated in the AFB1 group. Subsequently, lipid peroxidation was initiated and eventually led to ferroptosis. Similarly, Yuan et al. found that acrylamide leads to redox imbalance through dysregulation of the xCT-GSH-GPX4 signaling and finally causes ferroptosis (Yuan et al. 2022). FSP1, as a pivotal factor against ferroptosis in parallel to the classical pathway (Bersuker et al. 2019; Doll et al. 2019), was also vastly depleted by AFB1 in our experiments. These results suggest that AFB1 induced ferroptosis in the kidney of ducks.

An emerging number of investigations have found that NCOA4-mediated ferritinophagy affected intracellular iron homeostasis and played an essential role in ferroptosis (Fang et al. 2021). Li et al. discovered that nuclear receptor coactivator 4 (NCOA4) bound to FTH1 of ferritin and delivered ferritin to the lysosome for degradation and release of free iron, a process termed "ferritinophagy" (Santana-Codina et al. 2021). Intracellular iron level and ferritinophagy are regulated bidirectionally, and the level of NCOA4 is a central determinant of ferritinophagy flux (He et al. 2022). In this study, NCOA4 and FTH1 were upregulated in the
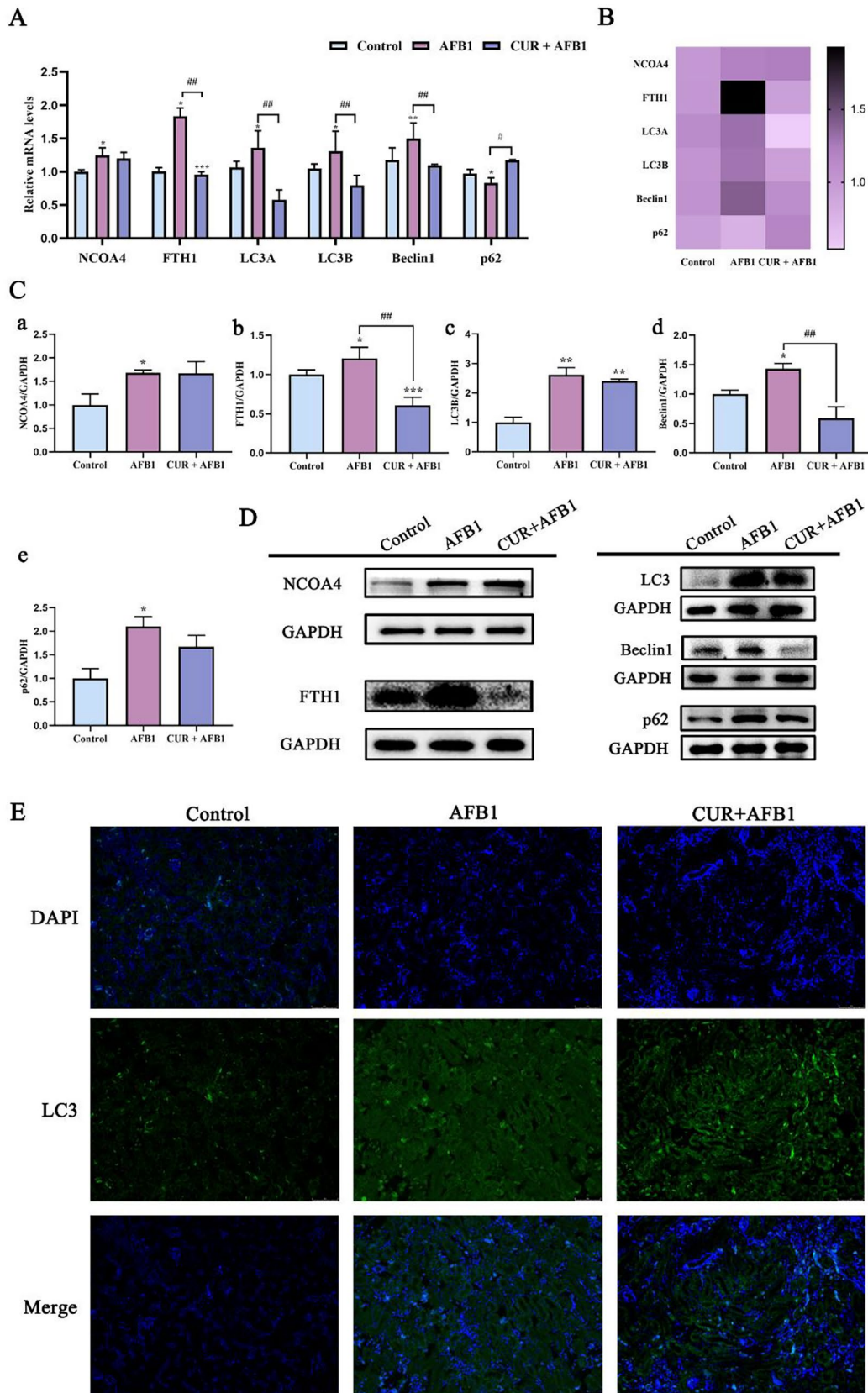
◀**Fig. 6** Effects of AFB1 exposure and CUR treatment on ferritin-ophagy. **A** mRNA levels of ferritinophagy-related genes. **B** Heatmap shows the correlation expression of ferritinophagy-related genes. **C** Quantification of protein levels of ferritinophagy-related genes. **D** Protein bands of ferritinophagy-related genes. **E** Immunofluorescence staining for LC3 in duck kidneys (×200). All data were expressed as mean±SEM; $n=6$ for each group. "*" indicates statistically significant difference from the control group ($*P<0.05$, $**P<0.01$, $***P<0.001$, and $****P<0.0001$). "#" means that the group is significantly different from the AFB1 group ($\#P<0.05$, $\#\#P<0.01$, $\#\#\#P<0.001$, and $\#\#\#\#P<0.0001$)

AFB1 group of ducks, which was in agreement with the trend of autophagy marker LC3B. Beclin1 and p62, participating in the conversion of primary autophagosomes to autophagosomes during ferritinophagy (Li et al. 2021), were also upregulated by AFB1. Accordingly, AFB1 can trigger ferroptosis in duck kidneys by activating NCOA4-mediated ferritinophagy.

In the present study, curcumin mitigated the accumulation of iron in renal tissues and also profoundly reversed the AFB1-induced alterations in ferroptosis corresponding factors (TF, TFR, ACSL4, COX2, NCOA4, FTH1, FTL, FSP1, GPX4), in our experiment. This may be partly due to the ability to bind metal ions and the strong iron chelating activity of curcumin (Bernabe-Pineda et al. 2004). Koonyosying et al. administered a green tea extract–curcumin drink to β-thalassemia patients to diminish redox-active iron and improve kidney function (Koonyosying et al. 2020). Rainey et al. noticed that iron chelation by curcumin suppressed autophagy and cell death of T51B and RL-34 epithelial cells (Rainey et al. 2019). Our study also illustrates that curcumin may inhibit ferroptosis by regulating iron metabolism, the system xc⁻/GSH/GPX4 axis, the PUFA pathway, and ferritinophagy, in which its antioxidant properties may play a key role. Astonishingly, several studies have illustrated that the Nrf2/HO-1 pathway was able to promote ferroptosis by liberating iron from heme (Fang et al. 2019; Hassannia et al. 2018; Jiang et al. 2021; Jing et al. 2022), which may also be one of the mechanisms by which curcumin relieves AFB1-induced ferroptosis in this study.

## Conclusion

In summary, this study reveals the mechanism of curcumin alleviating AFB1-induced kidney injury in ducks which is related to growth retardation, mitochondrial-mediated oxidative stress, and ferroptosis. However, curcumin suppresses AFB1-induced oxidative stress and ferroptosis by regulating the Nrf2 pathway and blocking NCOA4-induced ferritinophagy. This study provides strategies for treating various diseases caused by AFB1 poisoning from a new perspective.

## Declarations

## References

Adedara IA, Owumi SE (2023) Neurobehavioral and biochemical responses to artemisinin-based drug and aflatoxin B(1) co-exposure in rats. Mycotoxin Res 39:67–80

ALTamimi JZ, AlFaris NA, Al-Farga AM, Alshammari GM, Bin-Mowyna MN, Yahya MA (2021) Curcumin reverses diabetic nephropathy in streptozotocin-induced diabetes in rats by inhibition of PKCbeta/p(66)Shc axis and activation of FOXO-3a. J Nutr Biochem 87:108515

Bayir H, Dixon SJ, Tyurina YY, Kellum JA, Kagan VE (2023) Ferroptotic mechanisms and therapeutic targeting of iron metabolism and lipid peroxidation in the kidney. Nat Rev Nephrol 19:315–336

Benkerroum N (2020) Chronic and acute toxicities of aflatoxins: mechanisms of action. Int J Environ Res Public Health 17

Bernabe-Pineda M, Ramirez-Silva MT, Romero-Romo MA, Gonzalez-Vergara E, Rojas-Hernandez A (2004) Spectrophotometric and electrochemical determination of the formation constants of the complexes curcumin-Fe(III)-water and curcumin-Fe(II)-water. Spectrochim Acta A Mol Biomol Spectrosc 60:1105–1113

Bersuker K, Hendricks JM, Li Z, Magtanong L, Ford B, Tang PH, Roberts MA, Tong B, Maimone TJ, Zoncu R, Bassik MC, Nomura DK, Dixon SJ, Olzmann JA (2019) The CoQ oxidoreductase FSP1 acts parallel to GPX4 to inhibit ferroptosis. Nature 575:688–692

Chen GH, Song CC, Pantopoulos K, Wei XL, Zheng H, Luo Z (2022) Mitochondrial oxidative stress mediated Fe-induced ferroptosis via the NRF2-ARE pathway. Free Radical Biol Med 180:95–107

Chen X, Li J, Kang R, Klionsky DJ, Tang D (2021) Ferroptosis: machinery and regulation. Autophagy 17:2054–2081

Chuaysrinule C, Maneeboon T, Mahakarnchanakul W (2023) Mutual effects on mycotoxin production during co-culture of ochratoxigenic and aflatoxigenic Aspergillus strains. Mycotoxin Res 39:57–66

Dard L, Blanchard W, Hubert C, Lacombe D, Rossignol R (2020) Mitochondrial functions and rare diseases. Mol Aspects Med 71:100842

Deng D, Tang J, Liu Z, Tian Z, Song M, Cui Y, Rong T, Lu H, Yu M, Li J, Pang R, Ma X (2022) Functional characterization and whole-genome analysis of an aflatoxin-degrading Rhodococcus pyridinivorans strain. Biology-Basel 11.

Diaz GJ, Murcia HW (2019) An unusually high production of hepatic aflatoxin B1-dihydrodiol, the possible explanation for the high susceptibility of ducks to aflatoxin B1. Sci Rep 9:8010

Di Paola D, D'Amico R, Genovese T, Siracusa R, Cordaro M, Crupi R, Peritore AF, Gugliandolo E, Interdonato L, Impellizzeri D, Fusco R, Cuzzocrea S, Di Paola R (2022) Chronic exposure to vinclozolin induced fibrosis, mitochondrial dysfunction, oxidative stress, and apoptosis in mice kidney. Int J Mol Sci 23

Doll S, Freitas FP, Shah R, Aldrovandi M, Da SM, Ingold I, Goya GA, Xavier DST, Panzilius E, Scheel CH, Mourao A, Buday K, Sato M, Wanninger J, Vignane T, Mohana V, Rehberg M, Flatley A, Schepers A, Kurz A, White D, Sauer M, Sattler M, Tate EW, Schmitz W, Schulze A, O'Donnell V, Proneth B, Popowicz GM, Pratt DA, Angeli J, Conrad M (2019) FSP1 is a glutathione-independent ferroptosis suppressor. Nature 575:693–698

Fan RF, Tang KK, Wang ZY, Wang L (2021a) Persistent activation of Nrf2 promotes a vicious cycle of oxidative stress and autophagy inhibition in cadmium-induced kidney injury. Toxicology 464:152999

Fan T, Xie Y, Ma W (2021b) Research progress on the protection and detoxification of phytochemicals against aflatoxin B1-induced liver toxicity. Toxicon 195:58–68

Fang X, Wang H, Han D, Xie E, Yang X, Wei J, Gu S, Gao F, Zhu N, Yin X, Cheng Q, Zhang P, Dai W, Chen J, Yang F, Yang HT, Linkermann A, Gu W, Min J, Wang F (2019) Ferroptosis as a target for protection against cardiomyopathy. Proc Natl Acad Sci USA 116:2672–2680

Fang Y, Chen X, Tan Q, Zhou H, Xu J, Gu Q (2021) Inhibiting ferroptosis through disrupting the NCOA4-FTH1 interaction: a new mechanism of action. ACS Cent Sci 7:980–989

Fouche T, Claassens S, Maboeta M (2020) Aflatoxins in the soil ecosystem: an overview of its occurrence, fate, effects and future perspectives. Mycotoxin Res 36:303–309

Gao M, Yi J, Zhu J, Minikes AM, Monian P, Thompson CB, Jiang X (2019) Role of mitochondria in ferroptosis. Mol Cell 73:354–363

Gong Y, Hounsa A, Egal S, Turner PC, Sutcliffe AE, Hall AJ, Cardwell K, Wild CP (2004) Postweaning exposure to aflatoxin results in impaired child growth: a longitudinal study in Benin, West Africa. Environ Health Perspect 112:1334–1338

Gruber-Dorninger C, Jenkins T, Schatzmayr G (2019) Global mycotoxin occurrence in feed: a ten-year survey. Toxins 11

Guerrero-Hue M, Garcia-Caballero C, Palomino-Antolin A, Rubio-Navarro A, Vazquez-Carballo C, Herencia C, Martin-Sanchez D, Farre-Alins V, Egea J, Cannata P, Praga M, Ortiz A, Egido J, Sanz AB, Moreno JA (2019) Curcumin reduces renal damage associated with rhabdomyolysis by decreasing ferroptosis-mediated cell death. FASEB J 33:8961–8975

Hassannia B, Wiernicki B, Ingold I, Qu F, Van Herck S, Tyurina YY, Bayir H, Abhari BA, Angeli J, Choi SM, Meul E, Heyninck K, Declerck K, Chirumamilla CS, Lahtela-Kakkonen M, Van Camp G, Krysko DV, Ekert PG, Fulda S, De Geest BG, Conrad M, Kagan VE, Vanden BW, Vandenabeele P, Vanden BT (2018) Nano-targeted induction of dual ferroptotic mechanisms eradicates high-risk neuroblastoma. J Clin Invest 128:3341–3355

He J, Li Z, Xia P, Shi A, FuChen X, Zhang J, Yu P (2022) Ferroptosis and ferritinophagy in diabetes complications. Molecular Metabolism 60:101470

Jallow A, Xie H, Tang X, Qi Z, Li P (2021) Worldwide aflatoxin contamination of agricultural products and foods: from occurrence to control. Comprehensive Reviews in Food Science and Food Safety 20:2332–2381

Jiang X, Stockwell BR, Conrad M (2021) Ferroptosis: mechanisms, biology and role in disease. Nat Rev Mol Cell Biol 22:266–282

Jing S, Lu Y, Zhang J, Ren Y, Mo Y, Liu D, Duan L, Yuan Z, Wang C, Wang Q (2022) Levistilide a induces ferroptosis by activating the Nrf2/HO-1 signaling pathway in breast cancer cells. Drug Des Devel Ther 16:2981–2993

Koonyosying P, Tantiworawit A, Hantrakool S, Utama-Ang N, Cresswell M, Fucharoen S, Porter JB, Srichairatanakool S (2020) Consumption of a green tea extract-curcumin drink decreases blood urea nitrogen and redox iron in beta-thalassemia patients. Food Funct 11:932–943

Li H, Li S, Yang H, Wang Y, Wang J, Zheng N (2019a) l-proline alleviates kidney injury caused by AFB1 and AFM1 through regulating excessive apoptosis of kidney cells. Toxins 11

Li Q, Liao J, Chen W, Zhang K, Li H, Ma F, Zhang H, Han Q, Guo J, Li Y, Hu L, Pan J, Tang Z (2022) NAC alleviative ferroptosis in diabetic nephropathy via maintaining mitochondrial redox homeostasis through activating SIRT3-SOD2/Gpx4 pathway. Free Radical Biol Med 187:158–170

Li S, Muhammad I, Yu H, Sun X, Zhang X (2019b) Detection of aflatoxin adducts as potential markers and the role of curcumin in alleviating AFB1-induced liver damage in chickens. Ecotoxicol Environ Saf 176:137–145

Li W, Li W, Wang Y, Leng Y, Xia Z (2021) Inhibition of DNMT-1 alleviates ferroptosis through NCOA4 mediated ferritinophagy during diabetes myocardial ischemia/reperfusion injury. Cell Death Discovery 7:267

Liu J, Song WJ, Zhang NY, Tan J, Krumm CS, Sun LH, Qi DS (2017) Biodetoxification of aflatoxin B1 in cottonseed meal by fermentation of Cellulosimicrobium funkei in duckling diet. Poult Sci 96:923–930

Malir F, Pickova D, Toman J, Grosse Y, Ostry V (2023) Hazard characterisation for significant mycotoxins in food. Mycotoxin Res

Ma-On C, Sanpavat A, Whongsiri P, Suwannasin S, Hirankarn N, Tangkijvanich P, Boonla C (2017) Oxidative stress indicated by elevated expression of Nrf2 and 8-OHdG promotes hepatocellular carcinoma progression. Med Oncol 34:57

Mohajeri M, Behnam B, Cicero A, Sahebkar A (2018) Protective effects of curcumin against aflatoxicosis: a comprehensive review. J Cell Physiol 233:3552–3577

Nazhand A, Durazzo A, Lucarini M, Souto EB, Santini A (2020) Characteristics, occurrence, detection and detoxification of aflatoxins in foods and feeds. Foods 9

Oh SJ, Ikeda M, Ide T, Hur KY, Lee MS (2022) Mitochondrial event as an ultimate step in ferroptosis. Cell Death Discov 8:414

Qiao B, He Y, Gao X, Liu H, Rao G, Su Q, Ruan Z, Tang Z, Hu L (2023) Curcumin attenuates AFB1-induced duck liver injury by inhibiting oxidative stress and lysosomal damage. Food Chem Toxicol 172:113593

Rainey NE, Moustapha A, Saric A, Nicolas G, Sureau F, Petit PX (2019) Iron chelation by curcumin suppresses both curcumin-induced autophagy and cell death together with iron overload neoplastic transformation. Cell Death Discov 5:150

Ruan D, Zhu YW, Fouad AM, Yan SJ, Chen W, Zhang YN, Xia WG, Wang S, Jiang SQ, Yang L, Zheng CT (2019) Dietary curcumin enhances intestinal antioxidant capacity in ducklings via altering gene expression of antioxidant and key detoxification enzymes. Poult Sci 98:3705–3714

Rushing BR, Selim MI (2019) Aflatoxin B1: a review on metabolism, toxicity, occurrence in food, occupational exposure, and detoxification methods. Food Chem Toxicol 124:81–100

Santana-Codina N, Gikandi A, Mancias JD (2021) The role of NCOA4-mediated ferritinophagy in ferroptosis. Adv Exp Med Biol 1301:41–57

Wan F, Tang L, Rao G, Zhong G, Jiang X, Wu S, Huang R, Tang Z, Ruan Z, Chen Z, Hu L (2022) Curcumin activates the Nrf2

pathway to alleviate AFB1-induced immunosuppression in the spleen of ducklings. Toxicon 209:18–27

Wang P, Wang Y, Feng T, Yan Z, Zhu D, Lin H, Iqbal M, Deng D, Kulyar MF, Shen Y (2023) Hedyotis diffusa alleviate aflatoxin B1-induced liver injury in ducks by mediating Nrf2 signaling pathway. Ecotoxicol Environ Saf 249:114339

Wang X, Wang T, Nepovimova E, Long M, Wu W, Kuca K (2022a) Progress on the detoxification of aflatoxin B1 using natural anti-oxidants. Food Chem Toxicol 169:113417

Wang Y, Liu F, Zhou X, Liu M, Zang H, Liu X, Shan A, Feng X (2022b) Alleviation of oral exposure to aflatoxin B1-induced renal dysfunction, oxidative stress, and cell apoptosis in mice kidney by curcumin. Antioxidants 11

Wang Y, Song M, Wang Q, Guo C, Zhang J, Zhang X, Cui Y, Cao Z, Li Y (2022c) PINK1/Parkin-mediated mitophagy is activated to protect against AFB(1)-induced kidney damage in mice. Chem Biol Interact 358:109884

Xie J, Lv H, Liu X, Xia Z, Li J, Hong E, Ding B, Zhang W, Chen Y (2023) Nox4-and Tf/TfR-mediated peroxidation and iron overload exacerbate neuronal ferroptosis after intracerebral hemorrhage: involvement of EAAT3 dysfunction. Free Radical Biol Med 199:67–80

Yang WS, SriRamaratnam R, Welsch ME, Shimada K, Skouta R, Viswanathan VS, Cheah JH, Clemons PA, Shamji AF, Clish CB, Brown LM, Girotti AW, Cornish VW, Schreiber SL, Stockwell BR (2014) Regulation of ferroptotic cancer cell death by GPX4. Cell 156:317–331

Yu K, Zhang J, Cao Z, Ji Q, Han Y, Song M, Shao B, Li Y (2018) Lycopene attenuates AFB1-induced renal injury with the activation of the Nrf2 antioxidant signaling pathway in mice. Food Funct 9:6427–6434

Yuan Y, Yucai L, Lu L, Hui L, Yong P, Haiyang Y (2022) Acrylamide induces ferroptosis in HSC-T6 cells by causing antioxidant imbalance of the XCT-GSH-GPX4 signaling and mitochondrial dysfunction. Toxicol Lett 368:24–32

Zhao Y, Wang T, Li P, Chen J, Nepovimova E, Long M, Wu W, Kuca K (2021) Bacillus amyloliquefaciens B10 can alleviate aflatoxin B1-induced kidney oxidative stress and apoptosis in mice. Ecotoxicol Environ Saf 218:112286

Zhu YT, Wan C, Lin JH, Hammes HP, Zhang C (2022) Mitochondrial oxidative stress and cell death in podocytopathies. Biomolecules 12

Zhuang Y, Yang D, Shi S, Wang L, Yu M, Meng X, Fan Y, Zhou R, Wang F (2022) MiR-375-3p Promotes cardiac fibrosis by regulating the ferroptosis mediated by GPX4. Comput Intell Neurosci 2022:9629158